

ISAR Imaging Radar with Time-Domain High-Range Resolution Algorithms and Array Antenna

Christian Bouchard, étudiant 2^e cycle

Dr Dominic Grenier, directeur de recherche

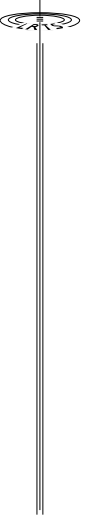
Abstract: To increase range resolution in ISAR imaging radar, time adaptations of the MUSIC algorithm and of Capon MLM are applied on each azimuth bin. The covariance matrix of each azimuth bin is estimated from the corresponding azimuth bin of ISAR images made with different carrier frequencies to avoid cross-correlation between scatterers. Simulation results are shown as well as some measurement processings.

Résumé: Pour augmenter la résolution en portée en imagerie radar ISAR, une adaptation en temps de l'algorithme MUSIC ou de la méthode du maximum de vraisemblance de Capon est appliquée sur chacun des azimuts. La matrice de covariance de chacun des azimuts est estimée à partir des azimuts correspondants d'images ISAR réalisées avec différentes fréquences porteuses pour éviter la corrélation croisée entre les réflecteurs. Des résultats de simulations de même que des traitements de mesures sont montrés.

Introduction

In the last few years, the ISAR-RMSA algorithm (Recursive Multiple-Scatterer algorithm) for imaging radar, based on the MSA algorithm [1], was developed at the Radiocommunication and Signal Processing Laboratory by H. Wu [2] and was improved to be used with an array antenna by Jean-René Larocque [3]. To increase the range resolution, we have applied time adaptations [4] of the MUSIC algorithm [5] and of Capon MLM [5] on each azimuth bin. The covariance matrix of each azimuth bin is estimated from the corresponding azimuth bin of ISAR images made with different carrier frequencies to avoid cross-correlation between target scatterers in the same cross-range bin.

In this text, we will discuss the time-domain high-range resolution algorithms and we will give the simulation parameters used and simulation results. Finally, processings of measurements done with a small radar are shown.



Time adaptations of the MUSIC algorithm and Capon MLM

The high-range resolution processing is done on each azimuth bin and it uses a time adaptation of MUSIC or Capon MLM which both need an estimation of the covariance matrix.

To do so, we make L images but we keep the complex data instead of keeping only the magnitude. The covariance matrix of each azimuth bin is estimated from the corresponding azimuth bin of the L images or snapshots. On an azimuth bin, the data in range for the l th image is :

$$r_l(t) = \sum_{k=1}^K \alpha_k e^{j2\pi f_l \tau_k} \Lambda_{2T_p}(t - \tau_k) + n_0(t), \quad (1)$$

where K is the number of scatterers on the azimuth bin, f_l is the carrier frequency used for the l th image, $\alpha_k = |\alpha_k| e^{j\phi_k}$ is proportional to the reflection coefficient of the k th scatterer, τ_k is the two-way travel time from the radar to this scatterer and $\Lambda_{2T_p}(t - \tau_k)$ is a triangular shape signal of duration $2T_p$ seconds centered at time τ_k , where T_p is the pulse length. Finally, $n_0(t)$ is an additive white gaussian noise.

To estimate the covariance matrix, the matrix containing the L snapshots is form :

$$\mathbf{X} = \begin{bmatrix} r_{1,1} & r_{2,1} & \cdots & r_{L,1} \\ r_{1,2} & r_{2,2} & \cdots & r_{L,2} \\ \cdots & \cdots & \cdots & \cdots \\ r_{1,M} & r_{2,M} & \cdots & r_{L,M} \end{bmatrix}, \quad (2)$$

$r_{l,m}$ is the complex image data of the m th range bin, l th image. The estimated covariance matrix is given by :

$$\hat{\mathbf{R}} = \frac{1}{L} \mathbf{X} \mathbf{X}^+ \quad (3)$$

where $^+$ is the complex transpose-conjugate operator. The eigenvectors and eigenvalues of $\hat{\mathbf{R}}$ can be found with singular value decomposition [5] for faster execution, that is $\hat{\mathbf{R}} = \mathbf{U} \mathbf{\Sigma} \mathbf{V}^+$. The eigenvectors are the column vectors of the matrix \mathbf{U} and the eigenvalues are $\lambda_l = \sigma_l^2 / L$ where σ_l is the l th singular value. The number of scatterers in the azimuth bin can be estimated by looking at the highest eigenvalues with a method such as the Akaike information criterion. After that, the signal and noise subspaces, \mathbf{P}_{sig} and \mathbf{P}_{n} can be form.

For projection, the complex exponentials of different frequencies of frequency-domain MUSIC and Capon are replaced by a complex signal model with different time delays :

$$\mathbf{s}_\tau = \begin{bmatrix} s_{1\tau} & s_{2\tau} & \cdots & s_{M\tau} \end{bmatrix}^T; s_{m\tau} = e^{j\frac{\pi}{4}} \Lambda_{2T_p/T_s}(m - \tau) \quad (4)$$

where a phase of $\pi/4$ radians is used so the projection will not be zero when either the in-phase signal or the quadrature signal is zero and T_s is the sampling interval. The delay estimation function of MUSIC, which consists of the inverse of the projection of the complex signal model into the noise subspace is :

$$\Phi_{\text{MU}}(\tau) = \frac{1}{s_{\tau}^+ \mathbf{P}_n s_{\tau}}, \quad 1 \leq \tau \leq M, \quad (5)$$

while Capon MLM is given by:

$$\Phi_{\text{ML}}(\tau) = \frac{1}{s_{\tau}^+ \hat{\mathbf{R}}^{-1} s_{\tau}}, \quad 1 \leq \tau \leq M \quad (6)$$

where :

$$\hat{\mathbf{R}}_{M \times M}^{-1} = \mathbf{U}_{M \times L} \mathbf{A}_{L \times L}^{-1} \mathbf{U}_{L \times M}^+ \quad (7)$$

in which $\mathbf{A}_{L \times L}$ is a diagonal matrix with the L eigenvalues on the diagonal. Φ should show peaks at the position of the scatterers.

Simulation

Now, it's time to look at the numerical results given by both high resolution algorithms. First, the simulation parameters are discussed and following that, images are shown.

Simulations parameters

The target and the trajectory geometries are shown in Figure 1 a). The biggest dots represent scatterers 10 dB above the noise, the medium dots, scatterers of the same intensity as the noise and the smallest dots, scatterers 10 dB under the noise. There is only one dominant scatterer that can be used to realize the focus, scatterer #1. The initial target range is $R = 20$ km and the target speed is constant at 250 m/s. The target travels at $\gamma = 50^\circ$ from the radar's initial LOS from an angle of arrival of $\alpha = 30^\circ$. We record 800 pulse returns for each image with an equivalent PRF of 400 Hz. The target aspect angle change is 1.017° and this gives a cross-range resolution of 1.543 m. The pulse length is 35 ns, the sampling interval is 3.5 ns and 77 samples are taken. The image cells are 0.525 m in range by 0.659 m in azimuth.

Simulations results

With those parameters, Figure 1 b) shows one of the low-resolution image before high-range resolution processing and Figure 2 a) shows the high-range resolution image made with MUSIC, $L = 8$ and a frequency step of 10 MHz. To resolve the scatterers with MUSIC, their signal-to-noise ratio after integration should be around 10 dB. The four corner points have a SNR of 0 dB, the SNR, after integration with $L = 8$, is around 9 dB which is enough to MUSIC to resolve them while the scatterers at -10 dB are not properly resolved.

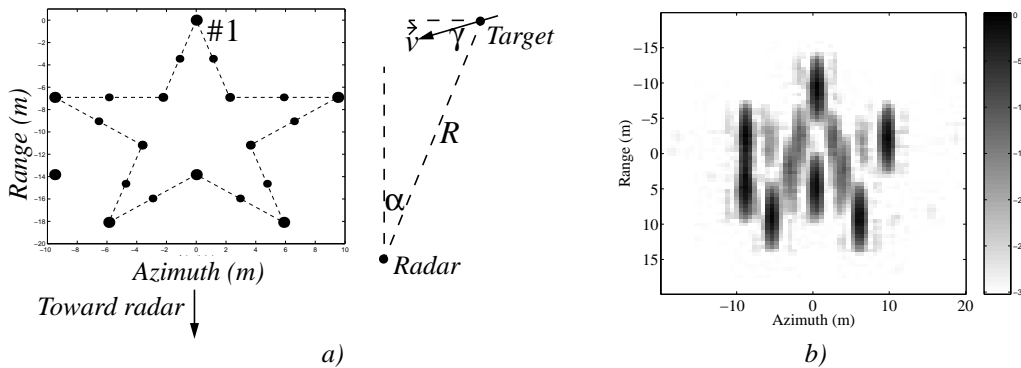
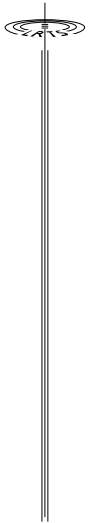


Figure 1 a) Target and trajectory geometries b) Low resolution image

The image in Figure 2 b) was also made with 8 low-resolution images but with only one carrier frequency. We see that on every azimuth bin having two strong scatterers, the projection is very low. As only one carrier frequency is used for the different snapshots, the phase shift between scatterers stays about the same, the sources are highly correlated so the rank of the matrix, which should be equaled to the number of sources, is reduced and the method do not work properly. The use of as many carrier frequencies as snapshots is one way to avoid this difficulty.

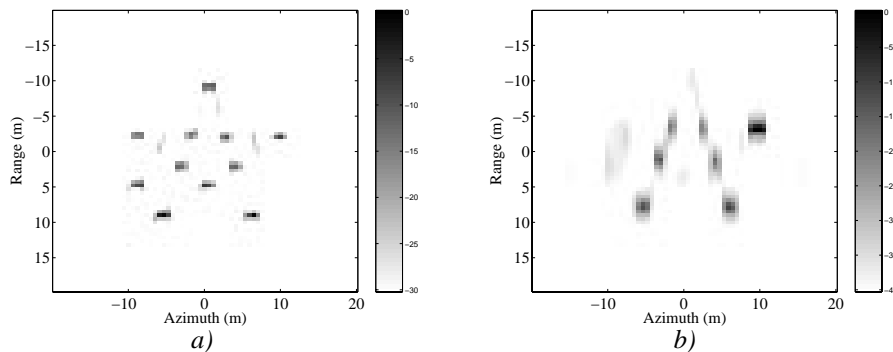


Figure 2 High-range resolution image made with MUSIC a) $L = 8$ carrier frequencies b) one carrier frequency

Measurement processings

To do the experiments, we have used the small radar made by Lab-Volt which uses a sub-sampling of 1024 pulse returns at a $PRF = 295$ kHz to recover one return. The pulse returns were sampled with an acquisition system made by Gagescope. For the high-range resolution signature, the target was stationary and made of a plexiglass plate in front of a metal plate. The distance between them was 9 cm. The pulse length was 2 ns, which, without processing, would give a Rayleigh resolution of 30 cm so the two scatterers cannot be resolved without pulse compression or processing.

Figure 3 a) shows a MUSIC high-resolution signature made with 16 snapshots and a fix carrier frequency of 9.4 GHz. The two scatterers are not resolved because of their cross-correlation. Figure 3 b) shows the signature of the same target, made with 16 snapshots but, this time, with carrier frequencies varying from 8.4 GHz to 9.9 GHz by 100 MHz steps. The two scatterers are resolved even though the distance between them is over estimated.

For high-range resolution ISAR images, 50 pulses were used and the initial range was 2.5 m. The parameters of Figure 1 were : $\gamma = 60^\circ$ and $\alpha = 3^\circ$, as the 3 dB antenna beamwidth is 6° this was the maximum value possible for α . We could not sampled the pulse returns with the target moving at a constant speed, so we positioned the target, sampled one pulse return, move the target, took another pulse return and so on. This was controled by the parallel port of the acquisition system. The equivalent target speed was 1.44 m/s with a PRF of 288 Hz. We repeated this process 16 times with different carrier frequencies to obtain 16 snapshots. Figure 4 a) shows the low-resolution image made with the first snapshot, the plate were 28 cm apart in the range distance and 8 cm apart in azimuth. The two scatterers are resolved in range. Figure 4 b) shows the MUSIC high-range resolution image. The distance between the scatterers is correctly evaluated.

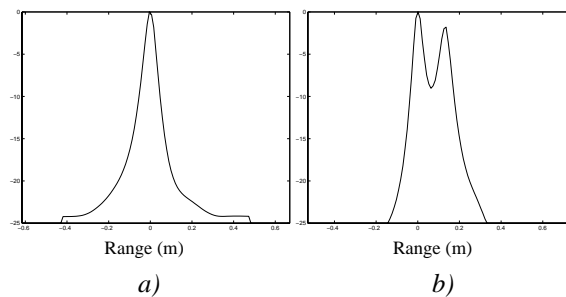


Figure 3 MUSIC High-resolution signatures of the target with a) one carrier frequency b) 16 carrier frequencies

Conclusion

The ISAR-RMSA imaging radar algorithm has been presented as the time-domain high-range resolution algorithms applied after cross-range processing. Simulations have shown the effect of the cross-correlation between the scatterers when only one carrier frequency was used and that a number of carrier frequencies equaled to the number of snapshots allowed the time-domain algorithms to work. A transmitted wide band signal received by an array in which the elements operate at different frequencies could also be used to get the snapshots. High-range resolution signatures and an high-range resolution ISAR image from radar measurements have been shown to demonstrate the usefulness of the method in practice.

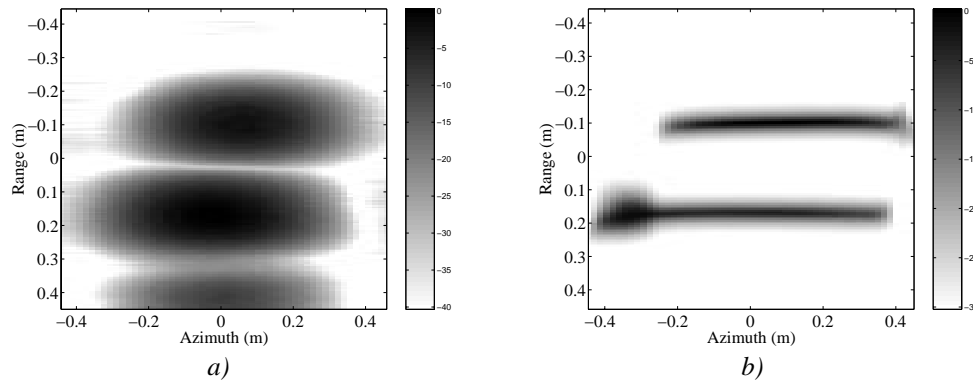
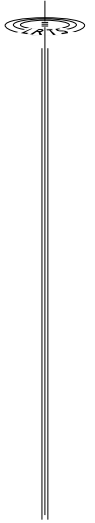


Figure 4 ISAR radar images a) image from the first snapshot b) MUSIC high-resolution image

Acknowledgements

This work was supported by NSERC and Canadian Space Agency scholarships. The computer program used to move the target along a specified trajectory and to sample the radar signal was done in collaboration with Jean-René Larocque.

References

- [1] B. D. Steinberg, H. M. Subbaram, *Microwave Imaging Techniques*. New York, John Wiley & Sons, inc, 1991.
- [2] H. Q. Wu, D. Grenier, G. Y. Delisle, D.-G. Fang, “Translational Motion Compensation in ISAR Image Processing”, *IEEE Trans. Image Proc.*, vol. 4, no. 11, pp.1561-1571, Nov. 1995.
- [3] J.-R. Larocque, D. Grenier, “Application of the new algorithm ISAR-GMSA to a linear phased array antenna”, in *Can. Conf. on Electr. and Comp. Eng.*, NF (CANADA), May 1997, pp. 351-354.
- [4] D. Grenier, É. Pigeon, R. M. Turner, “High-range resolution mono-frequency pulsed radar for the identification of approaching targets using subsampling and the MUSIC algorithm”, *IEEE signal proc. letters*, vol. 3 no. 6 June 1996.
- [5] C. W. Therrien, *Discrete Random Signals and Statistical Signal Processing*. Englewood Cliffs, NJ: Prentice-Hall, 1992.